Computational Materials Science 177 (2020) 109589

Contents lists available at ScienceDirect

Computational Materials Science

journal homepage: www.elsevier.com/locate/commatsci

Strain-induced novel properties of alloy nitride nanotubes

Naiara L. Marana[a], Giovanne B. Pinhal[a], José A.S. Laranjeira[a], Prescila G.C. Buzolin[a], Elson Longo[b], Julio R. Sambrano[a,*]

[a] Modeling and Molecular Simulation Group – CDMF, São Paulo State University, UNESP, Bauru, SP, Brazil
[b] CDMF, LIEC, Federal University of São Carlos, P.O. Box 676, São Carlos 13565-905, Brazil

ARTICLE INFO

Keywords:
Alloy nanotube
DFT
Piezoelectricity
Nitride nanotubes
Strain
Functionalization

ABSTRACT

Nanotubes have become the focus of interest in recent years because of their unique properties that make them natural candidates for many devices. The junction of two different nanotubes can form alloys imparting new properties or enhance existing properties associated with one or both starting materials. The present study aims to investigate the properties of aluminum and gallium nitride (AlN and GaN, respectively) single- and double-walled nanotubes and double-walled alloy nanotubes ($Al_{0.5}Ga_{0.5}N$ and $Ga_{0.5}Al_{0.5}N$) by using the density functional theory (DFT). It is observed that the emission of single-walled nanotubes (SWNT) changes from deep-UV to the blue region of the electromagnetic spectrum for double-walled GaN nanotubes (DWGaN). For the alloy nanotubes, the emission occurs at UVA and UVB regions for $Al_{0.5}Ga_{0.5}N$ and $Ga_{0.5}Al_{0.5}N$, respectively. Also, the impact of the applied mechanical strain is investigated for all nanotubes. It is observed that with tensile strain, the band gap energy decreases while the piezoelectricity increases. Of all the zigzag nanotubes investigated, SWAlN, DWAlN, and the $Al_{0.5}Ga_{0.5}N$ alloy nanotube exhibit larger piezoelectric constants. The analysis of electron density revels that the alloy nanotubes can be used to fabricate a selective dual gas sensor and that the functionalization, using an interface or by the application of strain, can be used to modulate the properties of materials.

1. Introduction

Nowadays, materials engineering is increasingly concerned with the development of new materials, as well as the functionalization of existing materials for application to specific devices. Functionalization can be achieved by doping, vacancies, adsorption, or by inducing defects in the crystal lattice, creating new materials that are more efficient than the starting materials. Another type of functionalization of current interest is the creation of a junction of two different materials in order to fabricate alloys. The alloys so obtained could either have very distinct properties or have similar, but significantly enhanced properties, as compared to the starting materials.

Among the different alloys, those of aluminum nitride (AlN) and gallium nitride (GaN), of the type GaN/AlN or $Al_xGa_{1-x}N$, are widely used in electronic devices [1–3]. Theoretical and experimental studies have shown that the aluminum content in these materials can be regulated to obtain higher efficiencies for applications in optoelectronic devices, in particular, those that utilize deep-UV radiation [4–7]. Furthermore, it was verified that the $Al_xGa_{1-x}N$ band gap energy depends on the thickness of the layer, as well as on the concentration of Al atoms [8,9]. Ambacher et al. [10], have established that the formation of the two-dimensional (2D) electron gas in non-doped GaN and AlGaN/GaN doped heterostructures depends both on the piezoelectric and spontaneous polarization effects. It has been shown that by introducing the piezotronics effect in the AlGaN/AlN/GaN heterostructure, the conductance increases up to 165% under compression along with an increase in the heterojunction electron gas, which has a wide application in high electron mobility transistors and other high-performance quantum electronics [11].

Despite many studies that report different GaN/AlN heterostructures, to the best of our knowledge, only a few correspond to one-dimensional (1D) materials, such as nanowires [12], nanorods [13], and nanotubes [14] that exhibit significant potential for applications in opto-electronics, magnetism, photonics, and catalysis [14,15]. The potential technological applications for nanotubes may be very different from those for which other 1D materials are natural candidates. In particular, nanotubes with small diameters serve as excellent high-performing structures that can be used as electrocatalysts, superconducting materials, in electrical devices, and in nano-sized sensors [16].

* Corresponding author.
E-mail address: jr.sambrano@unesp.br (J.R. Sambrano).

https://doi.org/10.1016/j.commatsci.2020.109589
Received 21 November 2019; Received in revised form 23 January 2020; Accepted 2 February 2020
Available online 15 February 2020

Detailed studies of inorganic nanotubes, among them, AlN and GaN nanotubes, began to advance, from the discovery of carbon nanotubes by Iijima et al. [17,18] The AlN and GaN nanotubes can be used in nanoscale photodetectors for the removal of toxic ethylene-acetylene gas from the environment and in formaldehyde sensors, in addition to having potential applications in the medical, electronic, optoelectronic, and piezoelectronic devices. Such broad-scale applicability can be attributed to their outstanding dielectric and piezoelectric properties, thermal conductivity, and possible quantum confinement effect [19–23].

Theoretical studies of AlN and GaN nanotubes highlight interesting properties, such as low strain energy involved in wrapping a surface to form a nanotube, good thermal stability, and increase in the band gap energy with increasing nanotube diameter, until a diameter of approximately 20 Å, when the band gap energy associated with the nanotube converges to that of the respective surface [24–27].

Although AlN and GaN nanotubes have shown great potential for various applications, very few studies have analyzed their synthesis, application, and functionalization. Furthermore, the nanotubes of AlN/GaN and $Al_xGa_{1-x}N$ heterostructures have not yet been synthesized. In fact, there is only one theoretical study by Almeida et al., wherein $Al_xGa_{1-x}N$ and GaN/$Al_xGa_{1-x}N$ nanotubes ($0 < x < 1$) [28] were investigated, in which it was shown that single-walled $Al_xGa_{1-x}N$ nanotubes displayed a direct band gap energy, with emission in the ultraviolet region for all concentrations of Al.

Modeling and computational simulations are fundamental tools for research in recent years, and can be used to model functionalized materials at the atomic level, as well as to predict their properties. As stated, the chemical bonds formed by the heterostructures significantly change the properties in comparison to that of the original material. Additionally, it is known that structural modifications produced by mechanical strain, as shown by Fabris et al. [29], increase the piezoelectricity, with a corresponding reduction in the band gap energy. The present study aims to theoretically analyze the main properties of the double-walled (DW) and alloy nanotubes, $Al_{0.5}Ga_{0.5}N$, and $Ga_{0.5}Al_{0.5}N$. In particular, the piezoelectricity and band gap energy were evaluated as a function of the simulated mechanical strain as applied along the periodic axis of the nanotubes. We also report an estimate of the mechanical limit of these structures as a function of tensile strain.

2. Method and computational details

2.1. Computational models

The theoretical equilibrium bulk structure of AlN and GaN, the (0001) surfaces and the single-walled nanotubes were previously studied, and the results can be found in reference [25]. The choice of the nanotube size originates from this study, in this sense, according to the low strain energy, which represents high stability of formation for nanotubes, the nanotubes with diameters of 20 Å were chosen. The computational setup and model system of this previous work allowed us to select the nanotube size (diameters of ~ 20 Å) to make a double-walled nanotube model. The alloy nanotube models were constructed from double-walled aluminum nitride nanotube by the substitution of Al by Ga atom, thus forming $Al_{0.5}Ga_{0.5}N$ or $Ga_{0.5}Al_{0.5}N$, depending on whether aluminum or gallium forms the inner layer of the nanotube. Fig. 1 shows the schematic representation of the construction of the nanotubes.

To measure the relative junction stability between AlN and GaN, the junction energy (E_{jun}) was determined using the relation $E_{jun} = (E_{@} - E_{GaN} - E_{AlN})/2S$, where $E_{@}$ corresponds to the alloy nanotube energy, the E_{GaN} and E_{AlN} are the energies that correspond to each wall of the alloy nanotube, calculated separately by removing the other wall, and S is the surface area of the alloy nanotube.

2.2. Computational method

Periodic computational simulations using Density Functional Theory (DFT) with the B3LYP [30] hybrid functional were made by using the CRYSTAL17 package [31]. The aluminum, gallium, and nitrogen atomic centers were described by 86-21G* [32], 86-4111d41G [33] and 6-21G* [34] all-electron basis sets, respectively. The functional and basis set choice is based on the results of previously published research [25,35]. The accuracy of the calculation was determined by a set of five-threshold values: 10^{-8}, 10^{-8}, 10^{-8}, 10^{-8} and 10^{-16}, which correspond, respectively, to the overlap and penetration of the Coulomb integrals, the overlap of the HF exchange integrals, with the last two values corresponding to the threshold for the pseudo-overlap in the HF exchange series. Also, the shrinking factor (Pack-Monkhorst and Gilat net) was set to 10, which corresponds to six independent k-points in the irreducible part of the Brillouin Zone integration.

The methodology for the calculations of elastic (c_{11}) and piezoelectric (e_{11}) constants, along the periodic direction of the nanotube was previously tested by our group and was shown to be in good agreement with experimental data [25,35–37].

The applied strain was taken to be along the periodic direction and simulates the mechanical influence on the piezoelectric constants and band gap energy, until the nanotube ruptures. Negative strain corresponds to compression, while positive strain corresponds to the tensile strain on the nanotube.

3. Results and discussion

3.1. Analysis of main properties

Table 1 lists the geometric parameters for all the nanotube models analyzed. It was observed that the DWNT maintain the geometrical characteristics of the correspondent SWNT and (0001) surfaces, with an average Al-N and Ga-N bond length of ~1.99 Å, Al-$\widehat{\mathbf{N}}$-Al and Ga-$\widehat{\mathbf{N}}$-Ga bond angle of ~127°, and nanotubes diameter of 18.84 Å and 19.50 Å of for DWAlN and DWGaN, respectively.

For alloys nanotubes, the higher diameter of $Ga_{0.5}Al_{0.5}N$, 19.38 Å, is due to the incorporation of Ga atoms in the internal wall, once the Ga-N bonds length and diameter are greater than Al-N. The Al-N = 2.02 Å and Ga-N = 2.10 Å bond lengths between walls are approximately the same for both alloy nanotubes. The calculated values for bond lengths and bond angles are found to be within the range reported for experimental and theoretical studies of these systems in the literature [2,5,38], and are similar to bulk and surfaces.

The E_{jun} values obtained for the alloy nanotubes were −0.0959 eV/unit and −0.0957 eV/unit for $Al_{0.5}Ga_{0.5}N$ and $Ga_{0.5}Al_{0.5}N$, respectively, which indicate good interaction between them, suggesting that, experimentally, each can form a good substrate for the other and, once synthesized, they will have small structural defects.

Interestingly, both the nanotube diameter and the wall thickness appear to affect the E_{gap}, as well as the emission range in the electromagnetic spectrum (*ERES*). Fig. 2 depicted the influence of the wall thickness and the composition in the alloy nanotube concerning the E_{gap}. As can be seen in Fig. 2, the SWNTs have higher values of E_{gap}, and by adding a second wall, E_{gap} decreases for the DWNTs, with values that are closer to the E_{gap} value of the corresponding bulk material. These results are in agreement with many theoretical and experimental works [5,39,40]. Park et al. [41] and Goldberger et al. [40] obtained values of E_{gap} between 3.2 and 3.9 eV for GaN nanotubes, and have demonstrated the effect of nanotube wall thickness on its electronic properties, once the structure starts to resemble the bulk structure. So far, the experimental determination of E_{gap} for the AlN nanotube has not been reported. However, many theoretical studies have reported a direct band gap energy for both single-walled and faceted AlN nanotubes, which were simulated at different levels of theory [15,25].

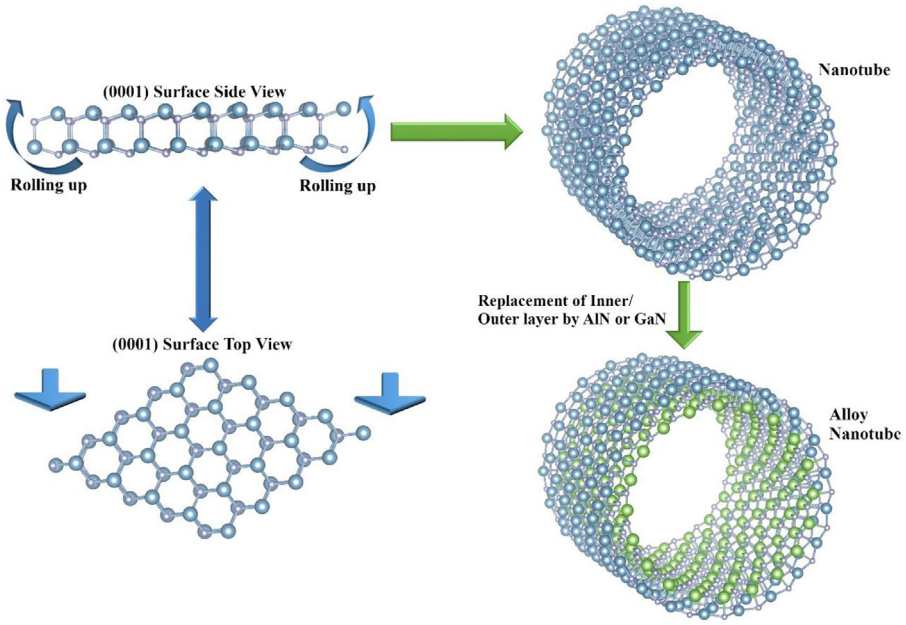

Fig. 1. Schematic representation of the construction of DW and alloy nanotubes.

Furthermore, it is known that the difference between the optical and electronic band gap energies is small [6], and so, the calculated theoretical band gap energy can be used to estimate the emission range of the nanotubes in the electromagnetic spectrum. The DWGaN is the only nanotube in this study with its emission in the visible region. For the $Al_{0.5}Ga_{0.5}N$ and $Ga_{0.5}Al_{0.5}N$ alloy nanotubes, the emission occurs at UVA and UVB regions, respectively. It is well-known that in AlN/GaN heterostructures the cation content is related to the photoluminescence (PL) emission, which increases with the percentage of Al in the sample [28,42,43]. In our models, the percentage of Al and Ga is 50% each; therefore, the change in the electromagnetic emission spectrum depends on which material is exposed, i.e., forms the outer layer of the DWNT. Park et al. [44] have experimentally demonstrated the relationship between the valence and conduction bands with respect to the exposed surface of GaN nanowires and nanotubes. Accordingly, DWNTs and alloy nanotubes can be used for different applications, such as deep-UV LEDs for water purification, medical diagnosis, ultraviolet A and B (UVA and UVB, respectively) radiation sensors based on photodiodes, among others [45].

The electronic properties were investigated by the calculation of the density of states (DOS), which can help to predict the main difference between the different types of nanotubes studied here. In Fig. 3 the DOS of DWNTs and alloy nanotubes are shown, and the main orbital contributors in each range are highlighted. For DWNTs, the electron transition probably occurs between the N-$2p_yp_z$ atom in the valence band (VB) and Al-*s* or Ga-*s* in the conduction band (CB), for DWAlN and DWGaN, respectively. The contributions found in the DOS of DWNTs is similar to the SWNTs, monolayer (0001) surface, as well as the respective GaN and AlN bulk. In the case of the alloy nanotubes, the

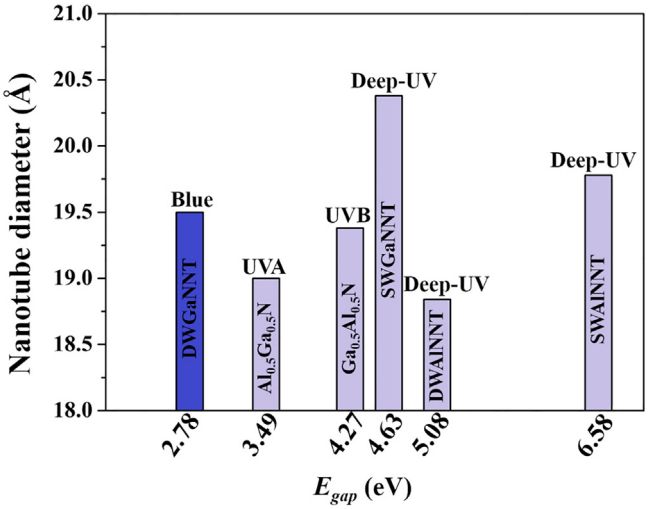

Fig. 2. Band gap energy (E_{gap}, eV) and emission range in the electromagnetic spectrum (*ERES*) as a function of nanotube diameters.

electron transition occurs between the atoms of the external wall, although the difference of internal/external wall contribution for N atoms in $Ga_{0.5}Al_{0.5}N$ is more pronounced. In this sense, for the $Ga_{0.5}Al_{0.5}N$ nanotube the electron transition occurs between N-$2p_yp_z$ and Al-*s*, while for the $Al_{0.5}Ga_{0.5}N$, the transition occurs between the N-$2p_yp_z$ and Ga-*s*. In both cases, the contribution of the cation-internal wall interaction appears above ~5 eV in the CB. Moreover, the E_{gap} of alloy nanotubes is

Table 1
Nanotube diameter (D; Å), bond length (X-N; Å) (X = Al or Ga) of the inner layer (in), outer layer (out) and between layers (bet) and bond angle X-$\hat{N}$-X (degree).

	D	X-N	X-N	$X\text{-}N_{(bet)}$	$X\text{-}N_{(bet)}$	X-$\hat{N}$-X	X-$\hat{N}$-X
SWAlN	19.78	1.79	–	–	–	119.75	–
SWGaN	20.38	1.84	–	–	–	119.72	–
DWAlN	18.84	$1.79_{(in)}$	$1.92_{(out)}$	2.01	2.02	$119.32_{(in)}$	$119.53_{(out)}$
DWGaN	19.50	$1.85_{(in)}$	$2.04_{(out)}$	2.13	2.12	$119.50_{(in)}$	$119.70_{(out)}$
$Ga_{0.5}Al_{0.5}N$	19.38	$1.84_{(in)}$	$2.03_{(out)}$	$2.02_{(N\text{-}Al)}$	$2.10_{(Ga\text{-}N)}$	$119.67_{(in)}$	$119.23_{(out)}$
$Al_{0.5}Ga_{0.5}N$	19.00	$1.81_{(in)}$	$1.99_{(out)}$	$2.13_{(N\text{-}Ga)}$	$2.05_{(Al\text{-}N)}$	$119.15_{(in)}$	$119.62_{(out)}$

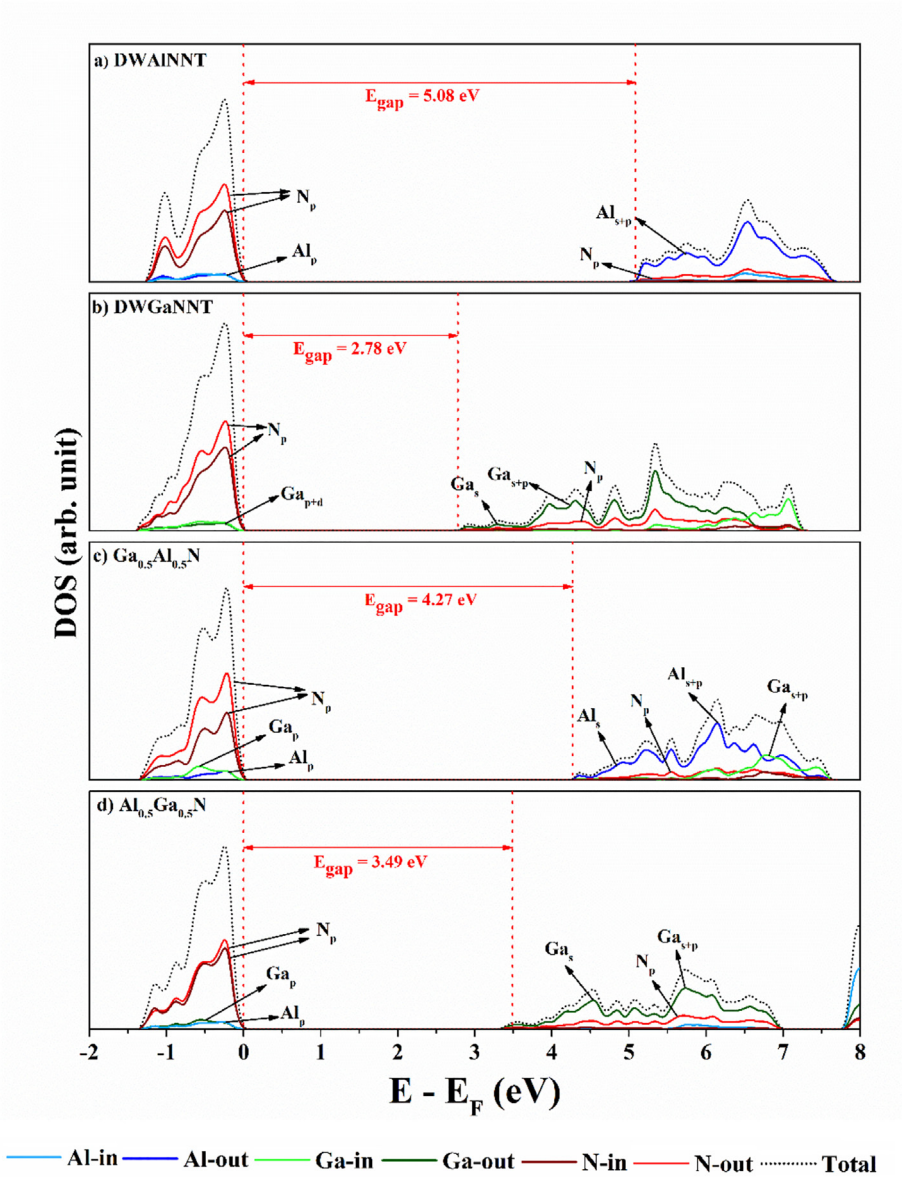

Fig. 3. Density of states for DWAlN, DWGaN, and $Ga_{0.5}Al_{0.5}N$ and $Al_{0.5}Ga_{0.5}N$ alloy nanotubes with respect to the inner and outer walls.

more affected by the AlN wall, as compared to that corresponding to the DWNTs, when the displacement of the AlN conduction band is ~1 eV to the forbidden region, i.e., closing the E_{gap}, whereas the displacement is minimum in the case of GaN.

The charge distribution on the isodensity surface based on the electronic charge density and the electrostatic potential of nanotubes is depicted in Fig. 4, with isolines being drawn at increments of 0.001 |e|/Å. The SWNTs and DWNTs show a homogeneous charge distribution (δ) along all the nanotube, as expected. The negative charge (δ^-) is more pronounced around N atoms in the GaN nanotubes, corresponding to a greater positive net charge (δ^+) on the Ga atoms than that on Al atoms, and is consistent with the charge density for SWNTs as calculated by Almeida et al. [28] However, when the interface AlN/GaN is formed, it was observed that charges flow in the Al to N direction, the nitrogen atom becomes more negative and the electron density is higher around the Al-N bond, for all the models analyzed here. The Mulliken charges are listed in Table S1 and validate the analyses described above. The difference found in the charge distribution for the alloy nanotubes can induce the adsorption or confinement of molecules. For example, for molecules that tend to withdraw electron density, the AlN nanotube is the more favorable adsorbent, such as NH_3 and NO_2, while for the molecules that tend to donate electronic density, the GaN nanotube is the preferred adsorbent, such as CH_3COOH and $C_6H_5COCH_3$.

The overlap population (see Table S2), based on Mulliken analysis, is an usual and simple method for describing electronic interactions between bonded atoms. The overlap values for $Al_{0.5}Ga_{0.5}N$ are 121 m|e| and 165 m|e|, for Ga-N and Al-N, respectively, whereas for $Ga_{0.5}Al_{0.5}N$, the overlap values are 138 m|e| and 131 m|e|, for Al-N and Ga-N, respectively. Once a high overlap population represents a greater covalent character of the bond, the results show that the Ga-N and Al-N bonds are more ionic compared with the single- and double-walled nanotubes, that have an overlap population of ~290 m|e| and ~298 m|e| for Al-N and Ga-N bonds, respectively. However, the Al-N bonds in all the models investigated here are seen to have a more pronounced covalent character, which might explain why the AlN nanotubes are observed to be more rigid than the GaN nanotubes, as indicated by their elastic constants listed in Table 2. These values are in good agreement with the bulk, (0001) surface and SW nanotube data [15,25,46]. In contrast to the electronic properties of the alloy nanotubes, the elastic constant is affected to a greater extent by the material

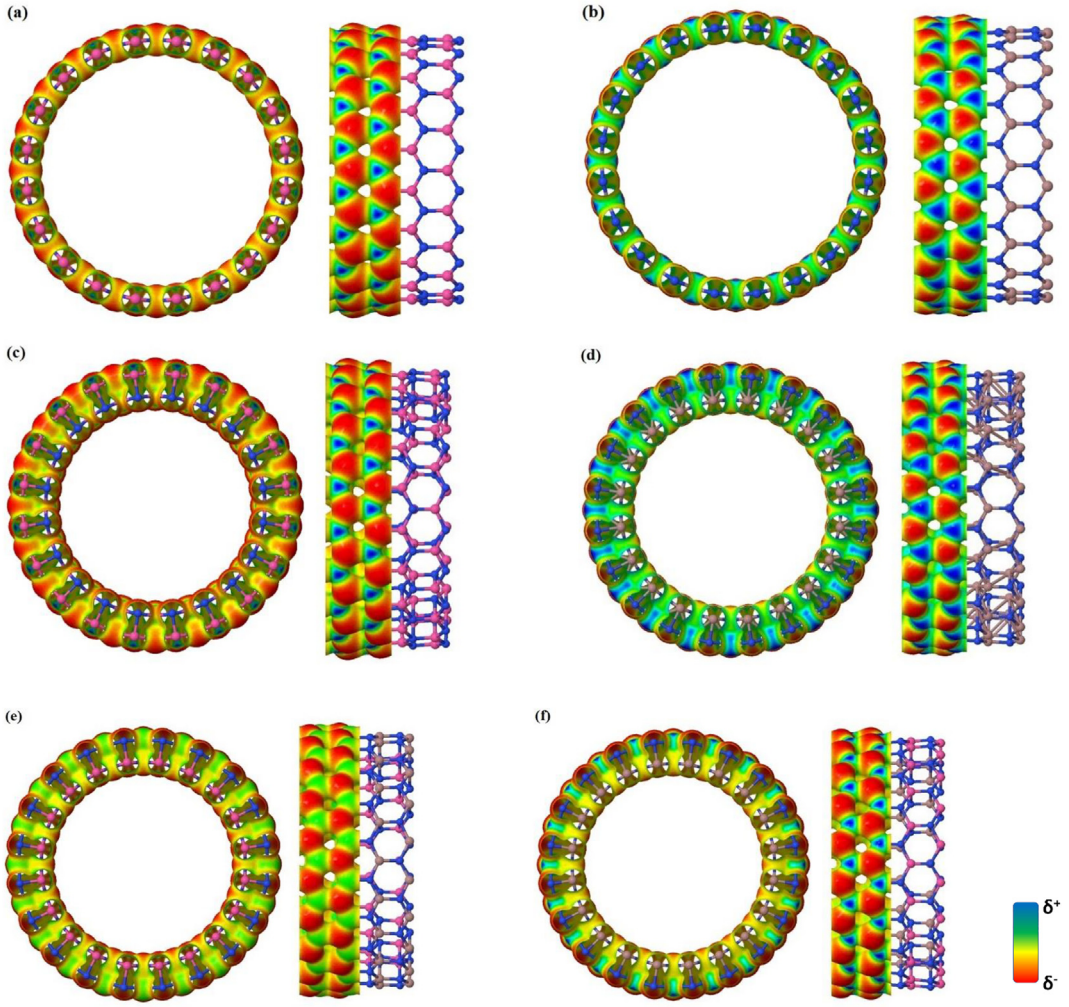

Fig. 4. Charge distribution on the isodensity surface of (a) SWAlN, (b) SWGaN, (c) DWAlN, (d) DWGaN, (e) $Al_{0.5}Ga_{0.5}N$ and (f) $Ga_{0.5}Al_{0.5}N$ nanotubes.

Table 2
Elastic (c_{11}, GPa) and piezoelectric (e_{11}, C/m^2) constants.

	c_{11}	e_{11}
SWAlN [25]	387.31	0.83
SWGaN [25]	367.46	0.62
DWAlN	351.61	0.14
DWGaN	311.48	0.08
$Ga_{0.5}Al_{0.5}N$	300.52	0.08
$Al_{0.5}Ga_{0.5}N$	321.19	0.11

which forms the internal wall of the nanotube. The rigidity of the inner wall adds to the rigidity of the nanotube. In this sense, the $Ga_{0.5}Al_{0.5}N$ nanotube is ~6.54% less rigid than $Al_{0.5}Ga_{0.5}N$, which corroborates with the above-mentioned hypothesis of the rigidity of the internal wall.

The addition of the outer wall in the nanotube appears to lead to a decrease in the piezoelectric properties (Table 2). Thus, the SWAlN and SWGaN are ~83% and 87%, respectively, more piezoelectric than the corresponding DWNTs. Unexpectedly, the alloy nanotubes seem to exhibit the low piezoelectricity observed in the DWNTs. When AlN, the most piezoelectric material among them [25,47,48], forms the inner wall of the nanotube, the piezoelectric constant of $Al_{0.5}Ga_{0.5}N$ nanotube is 21% lower than that for the DWAlN, but is seen to be 28% higher than the corresponding values for the DWGaN and $Ga_{0.5}Al_{0.5}N$ nanotubes. These results show that DWGaN, DWAlN and the corresponding alloy nanotubes are all piezoelectric, just like the SWNTs.

3.2. Strain versus piezoelectricity and band gap energy

One way to modify the material properties is by the application of mechanical strain. In this process, the structure is modified and it is known that these structural changes can regulate the properties of the material, and could also induce new properties hitherto not associated with the starting material. In order to investigate this, the mechanical strain was applied along the periodic axis of the nanotubes, which was varied between −20% to 24%, so as to analyze the maximum possible compression and stretch of the nanotube. The piezoelectric constants and band gap energy are shown in Fig. 5, as a function of the applied strain and the detailed results are given in the Supplemental Material (Tables S3–S5). Additionally, the nature of the bond (overlap population) as well as the Mulliken charges of the strained nanotubes were evaluated and are listed in Tables S6–S8.

As can be seen in Fig. 5, the SWNTs appear to be more sensitive to strain and the piezoelectric constants are found to oscillate. For all the nanotube models, the application of a compressive strain is seen to lead to a slight increase in the piezoelectric constant. Despite SWNTs are more rigid than DWNTs and the alloy nanotubes, all can be compressed until a limit of −12%, after which the piezoelectric constants were observed to start decreasing and the bonds Al-N and Ga-N become weaker. An abrupt decrease in piezoelectric constants is seen for a compressive strain of −16%. In the limit of compression, the overlap population is greater between the atoms and the bond character is altered. In all cases, the AlN and the $Al_{0.5}Ga_{0.5}N$ nanotubes appear to be

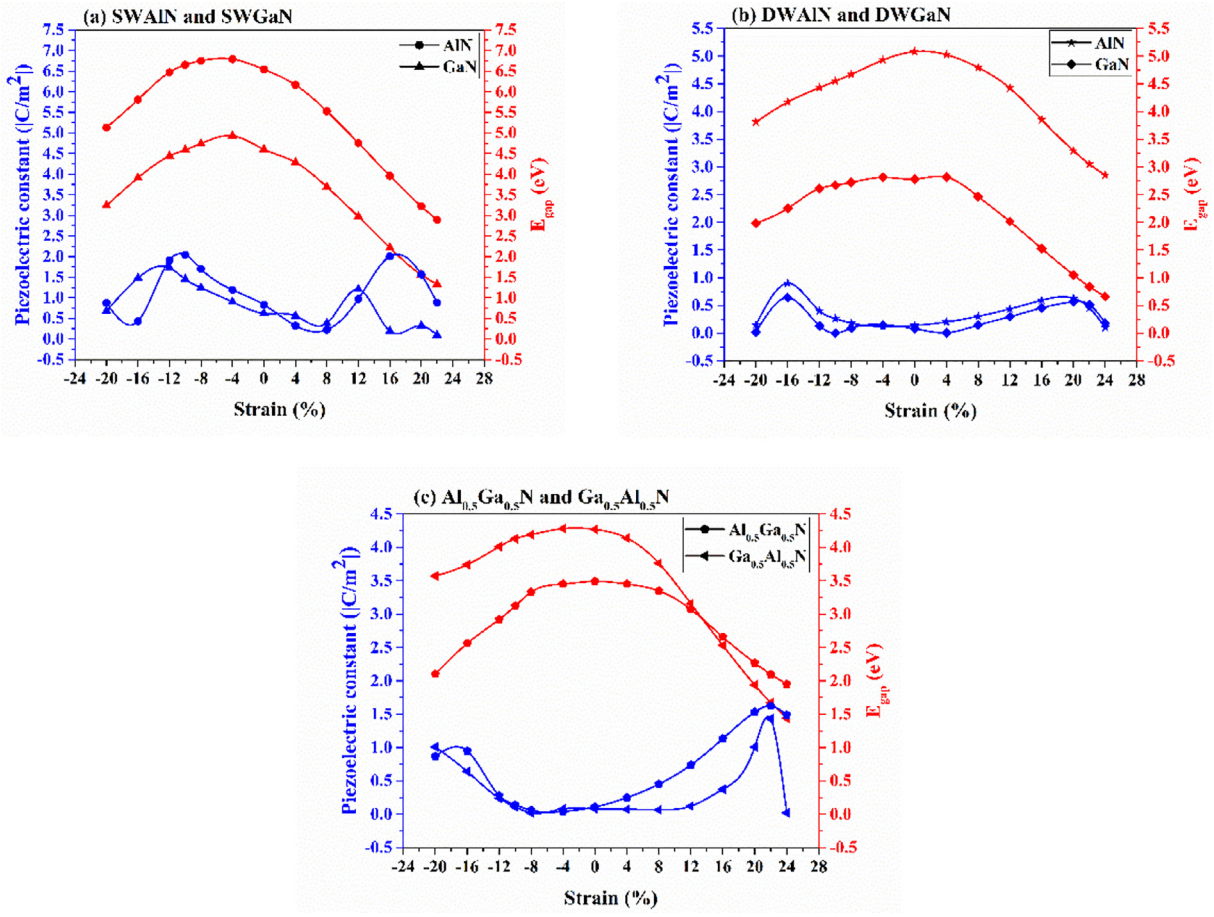

Fig. 5. Piezoelectric constants and band gap energy of (a) SW, (b) DW and (c) alloy nanotubes under compressive and tensile strain.

more resistant to the strain. This is consistent with the fact that AlN materials are more rigid, and the fact that Al constitutes the inner wall in the $Al_{0.5}Ga_{0.5}N$, which increases the rigidity of the alloy nanotube.

In contrast, the tensile strain affects the properties of the nanotubes to a greater extent. The SWNTs are found to exhibit a greater oscillation in piezoelectric constants, with the values being less than that of the unstrained nanotube, until a tensile strain of 8%. The piezoelectric constants increase significantly beyond a tensile strain of 12% for SWGaN, while such an increase for SWAlN only appears in response to a tensile strain of 16%. The present study indicates that 16% represents the limit of the tensile strain for both SWNTs, beyond which the nanotube starts to broken. The bond lengths of Ga-N and Al-N are found to be around 2.18 Å, which indicates that there is no chemical bond, but only an electrostatic interaction between a cation and an anion. The overlap population decreases potentially from this limit, indicating the change in the bond character (see Table S6).

In contrast to what is observed for the SWNTs, it was observed that the piezoelectric constant of DWAlN starts to increase beyond a tensile strain of 4%, while for DWGaN, this occurs from 8% onwards. The DWGaN exhibits a noteworthy increase in percentage in the piezoelectric constants, ~600%, and the value achieved is similar to that observed for the SWGaN (0.62C·m^2). It is seen that 20% is the limit of tensile strain for both DWNTs in this study, and at 22% tensile strain, the rupture of the nanotube occurs. However, the changes in the overlap population and Mulliken charges appear at 16% for DWAlN and only at 20% for DWGaN. This behavior is consistent with the softness of the GaN materials compared with AlN. Nevertheless, despite the rapid increase in piezoelectric constants given by tensile strain, the values did not permit the DWNTs to be classified as a good piezoelectric material.

The limit of tensile strain for the alloy nanotubes is taken to be 20%, since they are observed to rupture at a 22% tensile strain. The $Al_{0.5}Ga_{0.5}N$ is the most rigid nanotube and presents the higher increase in the piezoelectric constant before the rupture, with an increase of 1292% with respect to the unstrained nanotube, which makes it the most piezoelectric nanotube in the present study. For the alloy nanotubes, the piezoelectric properties depend on the material constituting the inner wall. Since the Al-N bond is seen to be sensitive to deformations, when the strain is applied, it creates a large tension on the AlN wall, which translates to an increase in piezoelectric constants. Additionally, it seems that in both alloy nanotubes the Al-N bond suffers more the tensile strain effect than Ga-N bonds. In this sense, the abrupt decrease in the properties is caused by changes in the overlap population of the Al-N bonds (of the wall and between them).

In all the models analyzed here, the applied strain leads to a decrease in E_{gap} values. However, as all nanotubes can be more stretched than compressed, the nanotubes exhibited smaller E_{gap} values when 8% of tensile strain (rather than 8% of compressive strain) was applied. For SWNTs, the band gap decreases by almost 35% before the nanotube ruptures, and the E_{gap} for both DWNTs decrease considerably with the tensile strain, which makes them more conducting than the SWNTs (both with and without strain), as well as the DWNTs (0% strain), the bulk material and (0001) monolayer surface. Consequently, the range of emission in the electromagnetic spectrum is also modified. The $Ga_{0.5}Al_{0.5}N$ nanotube was not the most piezoelectric nanotube, even after the application of tensile strain, but the reduction in E_{gap} was enough to change the emission in the electromagnetic spectrum, from UVB (0% strain) to blue (16% strain) and red (20% strain). These results suggest that structural manipulation can be used to modify the properties of materials.

Interesting, small changes were found in DOS analysis. As expected,

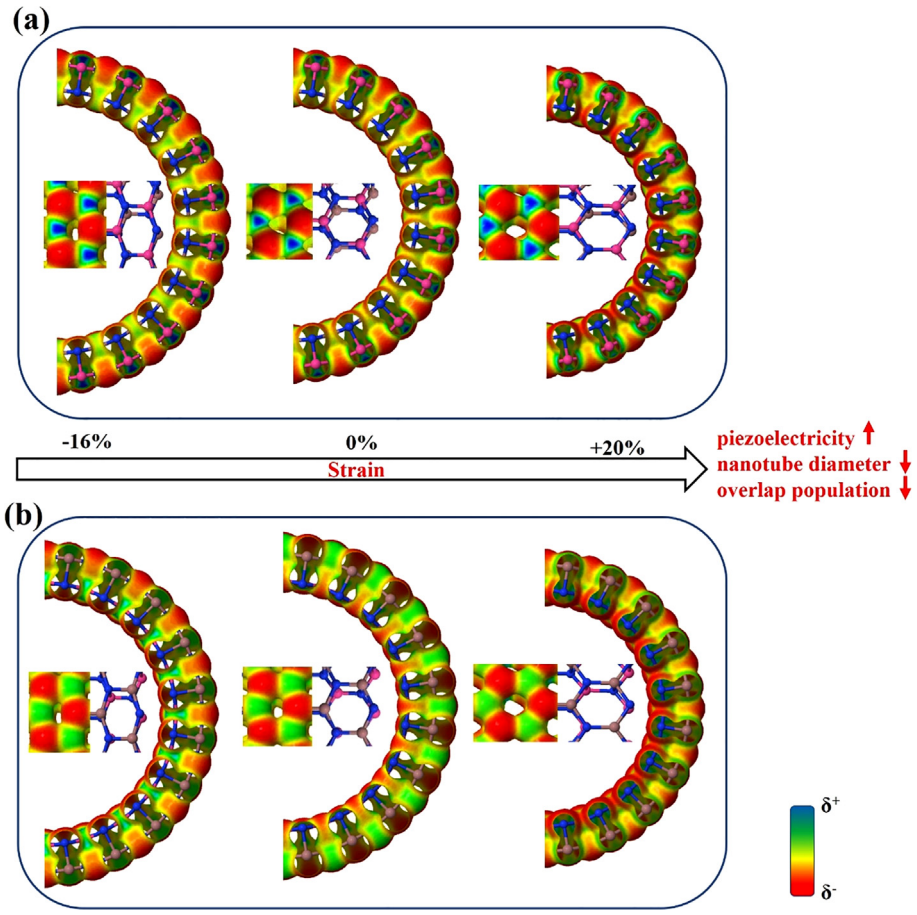

Fig. 6. Resume of the strain-induced properties for (a) $Ga_{0.5}Al_{0.5}N$ and (b) $Al_{0.5}Ga_{0.5}N$ nanotubes.

with the compression strain, the orbitals become more concentrated around the gap region, however, the main behavior of the contribution of the orbitals was not modified. The tensile strain alters the contribution of the s orbitals of the Al and Ga in the conduction band, closing the band gap. In special, the inner and outer layer of the DWNTs and alloy nanotubes have similar contribution of s orbital in the forbidden region.

To resume and clarify the effect of the strain in the alloy nanotubes properties, the charge distribution on the isodensity surface is depicted in Fig. 6. As can be seen, with the increase of the tensile strain, the nanotube diameter decrease, and the electronic density between the bonds become narrower, suggesting a weakening between the bonds. However, in both cases, the N atoms bonded with Al atoms have the more pronounced negative charges (as can be confirmed by Mulliken charges in Table S8). In contrast, with the compressive strain, the electronic density between the bonds are more scattered, indicating an increase in electron sharing between atoms.

In this sense, the piezoelectric properties of the nanotubes studied here can be efficiently increased with the application of tensile strain. The nitride nanotubes are known to be more resistant to the tensile strain, as compared to other materials, and the piezoelectric response attained with the application of tensile strain in this study is higher than that exhibited by DWZnONT, DWGaN, ZnO@GaN, and GaN@ZnO nanotubes [35], but is less than that exhibited by ZnO@GaN and GaN@ZnO nanotubes, when subjected to tensile strain.

4. Conclusions

DFT was used to theoretically investigate the properties of AlN and GaN nanotubes, as well as the $Al_{0.5}Ga_{0.5}N$ and $Ga_{0.5}Al_{0.5}N$ alloy nanotubes. The effect of strain applied along the periodic axis of nanotube on the piezoelectric constants and band gap energy was investigated. The single-walled nanotubes, both with and without application of the external strain, are found to be more piezoelectric than the double-walled nanotubes. Also, it was shown that all nanotubes respond satisfactorily to the tensile strain until ~16%. Without the external strain, the band gap energy of double-walled is reduced, by the addition of the second wall, in comparison with the single-walled nanotubes. The influence of the external wall is intensified when the alloy is constructed; thus, the alloy nanotube acquires the band gap energy value of the material that constitutes the outer layer. Additionally, the analyzed of the Mulliken charges of the alloy nanotubes showed that the charge is concentrate around Al-N bond, and this behavior can contribute to the rigidity of $Al_{0.5}Ga_{0.5}N$ nanotube. When the strain is applied, the band gap is altered and nanotubes are found to become more conducting, however no significant changes were found in DOS of the strained nanotubes. The present study clearly demonstrates that both, creation of an interface and application of an external strain, can be used to manipulate the material to enhance or modify selected properties. In this sense, with the alloy nanotubes, the difference in atomic charges between the walls can be used to fabricate a selective gas sensor. Also, the strained nanotube can be applied in some electronic device that requires a band gap energy of about 2.6 eV.

Credit authorship contribution statement

Naiara L. Marana: Conceptualization, Investigation, Methodology, Software, Validation, Formal analysis, Writing - original draft, Writing - review & editing. **Giovanne B. Pinhal:** Data curation, Formal analysis, Visualization. **José A.S. Laranjeira:** Data curation, Visualization.

Prescila G.C. Buzolin: Writing - original draft. **Elson Longo:** Funding acquisition. **Julio R. Sambrano:** Conceptualization, Funding acquisition, Investigation, Methodology, Project administration, Resources, Software, Supervision, Validation, Visualization, Writing - original draft, Writing - review & editing.

Declaration of Competing Interest

The authors declare that they have no known competing financial interests or personal relationships that could have appeared to influence the work reported in this paper.

Acknowledgements

This work was supported by the Brazilian Funding Agencies CAPES (grant no. 8881.068492/2014-01) and FAPESP (2013/07296-2, 2016/25500-4 and 2019/08928-9). The computational facilities were supported by resources supplied by Molecular Simulations Laboratory, São Paulo State University, Bauru, Brazil.

Appendix A. Supplementary data

Supplementary data to this article can be found online at https://doi.org/10.1016/j.commatsci.2020.109589.

References

[1] J. Zheng, L. Wang, X. Wu, Z. Hao, C. Sun, B. Xiong, Y. Luo, Y. Han, J. Wang, H. Li, J. Brault, S. Matta, M. Al Khalfioui, J. Yan, T. Wei, Y. Zhang, J. Wang, A PMT-like high gain avalanche photodiode based on GaN/AlN periodically stacked structure, Appl. Phys. Lett. (2016).
[2] H. Pan, Y.P. Feng, J. Lin, Electronic structures of AlGaN2 nanotubes and AlN-GaN nanotube superlattice, J. Chem. Theory Comput. (2008).
[3] G. Kipshidze, V. Kuryatkov, B. Borisov, S. Nikishin, M. Holtz, S.N.G. Chu, H. Temkin, Deep ultraviolet AlGaInN-based light-emitting diodes on Si(111) and sapphire, Phys. Status Solidi Appl. Res. (2002).
[4] Q. Li, P.K. Dasgupta, H. Temkin, M.H. Crawford, A.J. Fischer, A.A. Allerman, K.H.A. Bogart, S.R. Lee, Mid-ultraviolet light-emitting diode detects dipicolinic acid, Appl. Spectrosc. (2004).
[5] Y.F. Zhukovskii, A.I. Popov, C. Balasubramanian, S. Bellucci, Structural and electronic properties of single-walled AlN nanotubes of different chiralities and sizes, J. Phys. Condens. Matter. (2006).
[6] D. Bayerl, S. Islam, C.M. Jones, V. Protasenko, D. Jena, E. Kioupakis, Deep ultraviolet emission from ultra-thin GaN/AlN heterostructures Germanium-on-silicon nitride waveguides for mid-infrared integrated photonics Deep ultraviolet emission from ultra-thin GaN/AlN heterostructures, Cit. Appl. Phys. Lett. (2016).
[7] Sergey A. Nikishin, Mark Holtz, Henryk Temkin, Digital alloys of AlN/AlGaN for deep UV light emitting diodes, Jpn. J. Appl. Phys. 44 (10) (2005) 7221–7226, https://doi.org/10.1143/JJAP.44.7221.
[8] A. Pérez-Tomás, G. Catalàn, A. Fontserè, V. Iglesias, H. Chen, P.M. Gammon, M.R. Jennings, M. Thomas, C.A. Fisher, Y.K. Sharma, M. Placidi, M. Chmielowska, S. Chenot, M. Porti, M. Nafría, Y. Cordier, Nanoscale conductive pattern of the homoepitaxial AlGaN/GaN transistor, Nanotechnology (2015).
[9] Y. Taniyasu, M. Kasu, T. Makimoto, An aluminium nitride light-emitting diode with a wavelength of 210 nanometres, Nature (2006).
[10] O. Ambacher, J. Smart, J.R. Shealy, N.G. Weimann, K. Chu, M. Murphy, W.J. Schaff, L.F. Eastman, R. Dimitrov, L. Wittmer, M. Stutzmann, W. Rieger, J. Hilsenbeck, Two-dimensional electron gases induced by spontaneous and piezoelectric polarization charges in N- and Ga-face AlGaN/GaN heterostructures, J. Appl. Phys. 85 (1999) 3222–3233.
[11] X. Wang, R. Yu, C. Jiang, W. Hu, W. Wu, Y. Ding, W. Peng, S. Li, Z.L. Wang, Piezotronic effect modulated heterojunction electron gas in AlGaN/AlN/GaN heterostructure microwire, Adv. Mater. (2016).
[12] V. Piazza, A.V. Babichev, L. Mancini, M. Morassi, P. Quach, F. Bayle, L. Largeau, F.H. Julien, P. Rale, S. Collin, J.C. Harmand, N. Gogneau, M. Tchernycheva, Investigation of GaN nanowires containing AlN/GaN multiple quantum discs by EBIC and CL techniques, Nanotechnology (2019).
[13] Y.B. Tang, Z.H. Chen, H.S. Song, C.S. Lee, H.T. Cong, H.M. Cheng, W.J. Zhang, I. Bello, S.T. Lee, Vertically aligned p-type single-crystalline GaN nanorod arrays on n-type Si for heterojunction photovoltaic cells, Nano Lett. (2008).
[14] M. Law, J. Goldberger, P. Yang, Semiconductor nanowires and nanotubes, Annu. Rev. Mater. Res. 34 (2004) 83–122.
[15] R.A. Evarestov, Theoretical modeling of inorganic, Nanostructures (2015).
[16] C. Koenigsmann, M.E. Scofield, H. Liu, S.S. Wong, Designing enhanced one-dimensional electrocatalysts for the oxygen reduction reaction: probing size- and composition-dependent electrocatalytic behavior in noble metal nanowires, J. Phys. Chem. Lett. (2012).
[17] S. Iijima, Helical microtubules of graphitic carbon, Nature (1991).
[18] S. Iijima, T. Ichihashi, Single-shell carbon nanotubes of 1-nm diameter, Nature (1993).
[19] Y. Arakawa, Progress in GaN-based quantum dots for optoelectronics applications, IEEE J. Sel. Top. Quant. Electron. (2002).
[20] A. Ahmadi Peyghan, A. Omidvar, N.L. Hadipour, Z. Bagheri, M. Kamfiroozi, Can aluminum nitride nanotubes detect the toxic NH 3 molecules? Phys. E Low-Dimension. Syst. Nanostruct. (2012).
[21] M. Noei, A.A. Salari, N. Ahmadaghaei, Z. Bagheri, A.A. Peyghan, DFT study of the dissociative adsorption of HF on an AlN nanotube, Comptes Rendus Chim. (2013).
[22] H. Li, C. Liu, G. Liu, H. Wei, C. Jiao, J. Wang, H. Zhang, D.D. Jin, Y. Feng, S. Yang, L. Wang, Q. Zhu, Z.G. Wang, Single-crystalline GaN nanotube arrays grown on c-Al2O 3 substrates using InN nanorods as templates, J. Cryst. Growth (2014).
[23] H. Morkoç, S. Strite, G.B. Gao, M.E. Lin, B. Sverdlov, M. Burns, Large-band-gap SiC, III-V nitride, and II-VI ZnSe-based semiconductor device technologies, J. Appl. Phys. (1994).
[24] M. Zhao, Y. Xia, D. Zhang, L. Mei, Stability and electronic structure of AlN nanotubes, Phys. Rev. B – Condens. Matter Mater. Phys. (2003).
[25] G.B. Pinhal, N.L. Marana, G.S.L. Fabris, J.R. Sambrano, Structural, electronic and mechanical properties of single-walled AlN and GaN nanotubes via DFT/B3LYP, Theor. Chem. Acc. (2019).
[26] S.M. Lee, Y.H. Lee, Y.G. Hwang, J. Elsner, D. Porezag, T. Frauenheim, Stability and electronic structure of GaN nanotubes from density-functional calculations, Phys. Rev. B - Condens. Matter Mater. (1999).
[27] M. Zhao, Y. Xia, Z. Tan, X. Liu, F. Li, B. Huang, Y. Ji, L. Mei, Strain energy and thermal stability of single-walled aluminum nitride nanotubes from first-principles calculations, Chem. Phys. Lett. (2004).
[28] J.M. de Almeida, T. Kar, P. Piquini, AlN, GaN, AlxGa1 - xN nanotubes and GaN/AlxGa1 - xN nanotube heterojunctions, Phys. Lett. Sect. A Gen. At Solid State Phys. (2010).
[29] G.S.L. Fabris, N.L. Marana, E. Longo, J.R. Sambrano, Piezoelectric response of porous nanotubes derived from hexagonal boron nitride under strain influence, ACS Omega (2018).
[30] A.D. Becke, Density functional thermochemistry. 3. The role of the exact exchange, J. Chem. Phys. 98 (1993) 5648–5652.
[31] R. Dovesi, A. Erba, R. Orlando, C.M. Zicovich-Wilson, B. Civalleri, L. Maschio, M. Rérat, S. Casassa, J. Baima, S. Salustro, B. Kirtman, Quantum-mechanical condensed matter simulations with CRYSTAL, Wiley Interdiscip, Rev. Comput. Mol. Sci. (2018).
[32] B. Montanari, B. Civalleri, C.M. Zicovich-Wilson, R. Dovesi, Influence of the exchange-correlation functional in all-electron calculations of the vibrational frequencies of corundum (α-Al 2O3), Int. J. Quant. Chem. (2006).
[33] R. Pandey, J.E. Jaffe, N.M. Harrison, Ab initio study of high pressure phase transition in GaN, J. Phys. Chem. Solids. 55 (1994) 1357–1361.
[34] R. Dovesi, M. Causa, R. Orlando, C. Roetti, V.R. Saunders, Ab initio approach to molecular crystals: a periodic Hartree-Fock study of crystalline urea, J. Chem. Phys. 92 (1990) 7402–7411.
[35] N.L. Marana, S. Casassa, E. Longo, J.R. Sambrano, Computational simulations of ZnO@GaN and GaN@ZnO core@shell nanotubes, J. Solid State Chem. (2018).
[36] G.S.L. Fabris, N.L. Marana, E. Longo, J.R. Sambrano, Theoretical study of porous surfaces derived from graphene and boron nitride, J. Solid State Chem. 258 (2018) 247–255.
[37] N.L. Marana, S.M. Casassa, J.R. Sambrano, Piezoelectric, elastic, Infrared and Raman behavior of ZnO wurtzite under pressure from periodic DFT calculations, Chem. Phys. 485–486 (2017) 98–107.
[38] E.A. Pentaleri, V.A. Gubanov, C. Boekema, C.Y. Fong, First-principles band-structure calculations of p- and n-type substitutional impurities in zinc-blende aluminum nitride, Phys. Status Solidi Basic Res. (1997).
[39] D.C. Camacho-Mojica, F. López-Urías, GaN Haeckelite single-layered nanostructures: monolayer and nanotubes, Sci. Rep. (2015).
[40] J. Goldberger, R. He, Y. Zhang, S. Lee, H. Yan, H.J. Choi, P. Yang, Single-crystal gallium nitride nanotubes, Nature (2003).
[41] Y.S. Park, G. Lee, M.J. Holmes, C.C.S. Chan, B.P.L. Reid, J.A. Alexander-Webber, R.J. Nicholas, R.A. Taylor, K.S. Kim, S.W. Han, W. Yang, Y. Jo, J. Kim, H. Im, Surface-effect-induced optical bandgap shrinkage in GaN nanotubes, Nano Lett. (2015).
[42] Y. Taniyasu, M. Kasu, Polarization property of deep-ultraviolet light emission from C-plane AlN/GaN short-period superlattices, Appl. Phys. Lett. (2011).
[43] S.M. Islam, K. Lee, J. Verma, V. Protasenko, S. Rouvimov, S. Bharadwaj, H. Xing, D. Jena, MBE-grown 232-270 nm deep-UV LEDs using monolayer thin binary GaN/AlN quantum heterostructures, Appl. Phys. Lett. (2017).
[44] P.L. McEuen, J.-Y. Park, Electron transport in single-walled carbon nanotubes, MRS Bull. 29 (2004) 272–275.
[45] J. Theyirakumar, G. Gopir, B. Yatim, H. Sanusi, P.S. Megat Mahmud, T.C. Hoe, Testing and calibration of an ultraviolet-A radiation sensor based on GaN photodiode, Sains Malaysiana (2011).
[46] K. Kim, W.R.L. Lambrecht, B. Segall, Elastic constants and related properties of tetrahedrally bonded BN, AlN, GaN, and InN, Phys. Rev. B – Condens. Matter Mater. Phys. (1996).
[47] M.N. Blonsky, H.L. Zhuang, A.K. Singh, R.G. Hennig, Ab Initio prediction of piezoelectricity in two-dimensional materials, ACS Nano (2015).
[48] K. Shimada, First-principles determination of piezoelectric stress and strain constants of wurtzite III-V nitrides, Jpn. J. Appl. Physics Part 2 Lett. (2006).